PAPER

Check for updates

Ghatti gum-base graft copolymer: a plausible platform for pH-controlled delivery of antidiabetic drugs

Rohit R. Bhosale,[a] Riyaz Ali M. Osmani,[b] Amr S. Abu Lila, [ID][cd] El-Sayed Khafagy,[ef] Hany H. Arab,[g] Devegowda V. Gowda,[h] Mohamed Rahamathulla,[i] Umme Hani,[i] Mohd Adnan[j] and Hosahalli V. Gangadharappa [ID] *[h]

In the present study, we aimed to develop a novel pH-sensitive polymeric delivery system (GG-*g*-PMMA) for antidiabetic therapy *via* grafting ghatti gum (GG) with methyl methacrylate (MMA) chains. The free radical polymerization technique was adopted to graft ghatti gum with methyl methacrylate, using ceric ammonium nitrate (CAN) as a redox initiator. The impact on grafting parameters such as grafting percentage (*G*%) and grafting efficiency (GE), of monomer and initiator concentrations was evaluated. The batch with higher grafting efficiency and percentage grafting was selected and characterized by elemental analysis (C, H and N), DSC, FT-IR spectroscopy, XRD, ^{1}H-NMR and SEM morphology study. In addition, the efficacy of GG-*g*-PMMA-based pellets loaded with the hypoglycemic agent, metformin hydrochloride, to sustain drug release was investigated. *In vitro* release studies demonstrated a pH-dependent sustained release of the drug from GG-*g*-PMMA pellets. In addition, acute oral toxicity studies and histopathological analysis suggested the safety and biocompatibility of the grafted gum. Most importantly, *in vivo* efficacy studies underscored the efficient hypoglycemic potential of the prepared formulation, which was comparable to that of a sustained release marketed formulation. These results suggest that the developed pH-sensitive polymeric delivery system (GG-*g*-PMMA) might represent a promising delivery vehicle for facilitated antidiabetic therapy.

1. Introduction

Natural polymers have been extensively utilized as vehicles for the entrapment and delivery of drugs.[1,2] Compared to synthetic polymers, natural polymers show superiority in the biocompatibility, biodegradability and easy accessibility.[1,3] Furthermore, the presence of reactive groups on the native natural polymers enables the interaction with other functional groups. Such modification bestows the newly obtained polymer with tremendous functions and/or alters their physical and chemical properties.[4,5]

Gum ghatti (GG) or Indian gum is an example of natural polymers that that has been extensively used in food, pharmaceuticals and other industries due to its superior thickening and emulsification properties.[6,7] GG is a translucent amorphous exudate of *Anogeissus latifolia* tree; a large deciduous tree grown in dry areas. It is a complex non-starch polysaccharide composing of D-mannose, D-galactose, L-arabinose, and D-glucuronic acid.[6] Recently, GG has been investigated as a new release modifier in the formulation of matrix tablets.

Modification of natural polymers by graft copolymerization techniques has received tremendous attention.[8–10] This method allows the grafting of one or more blocks of homopolymer with a variety of functional groups onto the backbone of the main chain, thus altering the physical and chemical properties of original grafted polymer.[9,11] There are three main approaches for graft polymerization; grafting to, grafting from, and grafting through methods. The "grafting to" approach comprises the coupling of pre-formed polymer onto the surface by exploiting

[a]Department of Pharmaceutics, Krishna Institute of Pharmacy, Krishna Institute of Medical Sciences Deemed to be University, Karad-415539, Maharashtra, India

[b]Department of Biosciences and Bioengineering, Indian Institute of Technology Bombay (IITB), Mumbai-400076, Maharashtra, India. E-mail: riyazosmani@iitb.ac.in

[c]Department of Pharmaceutics and Industrial Pharmacy, Faculty of Pharmacy, Zagazig University, Zagazig-44519, Egypt. E-mail: a.abulila@uoh.edu.sa

[d]Department of Pharmaceutics, College of Pharmacy, University of Hail, Hail-81442, Saudi Arabia

[e]Department of Pharmaceutics, College of Pharmacy, Prince Sattam Bin Abdulaziz University, Al-Kharj-11942, Saudi Arabia

[f]Department of Pharmaceutics and Industrial Pharmacy, Faculty of Pharmacy, Suez Canal University, Ismailia-41552, Egypt

[g]Department of Pharmacology and Toxicology, College of Pharmacy, Taif University, Taif-21944, Saudi Arabia

[h]Department of Pharmaceutics, JSS College of Pharmacy, JSS Academy of Higher Education and Research, Mysuru, Karnataka, 570015, India. E-mail: hvgangadharappa@jssuni.edu.in

[i]Department of Pharmaceutics, College of Pharmacy, King Khalid University, Guraiger, Abha, 62529, Saudi Arabia

[j]Department of Biology, College of Science, University of Hail, Hail-2440, Saudi Arabia

the functional groups of both the surface and pre-formed polymer. The "grafting from" approach utilizes pre-attached precursors/initiators on the surface, which are subsequently used in polymerization reaction. In "grafting through" approach, a monomer of a lower molecular weight is radically copolymerized with an acrylate functionalized macromonomer.[8–10]

Generally, graft copolymerization process involves the use of an external agent capable of generating free radical sites on the backbone of the main polymer chains. After creation of free radical sites, one or more blocks of homopolymer are attached through chain propagation to the polymer backbone, thus forming the grafted chains.[11] Free radicals can be produced in a number of ways, usually involving separate initiator molecules. Ceric ammonium nitrate (CAN)-mediated free radical polymerization reaction is one of the most efficient, reproducible and less time-consuming methods for the synthesis of graft copolymers, which can be used in the formulation of sustained release as well as pH-sensitive drug delivery systems.[10,12]

pH-Sensitive drug delivery systems represent one of the most widely investigated stimuli-responsive drug delivery systems. They are designed to respond to a specific pH range at the site of action and to deliver the payload at specific time, resulting in enhanced therapeutic efficacy and patient compliance.[13,14] pH-Sensitive drug delivery systems showed favorable efficacies in certain disease conditions including peptic ulcers, diabetes, asthma, cardiovascular diseases and cancer.[15–19] Recently, many polymers/graft copolymers with pH responsiveness were successfully employed for the development of pH-sensitive drug delivery systems.

Metformin HCl, a biguanide derivative, represents the preferred first-line oral blood glucose-lowering agent to manage type 2 diabetes. It plays three primary roles: slowing the absorption of sugar into the small intestine, preventing the liver from dumping more glucose into the blood, and ultimately assisting the body to use natural insulin efficiently. Consequently, it lowers endogenous glucose production and does not cause overt hypoglycemia.[20,21] However, due to its hydrophilic nature, it is absorbed partially and slowly by the gastrointestinal tract, resulting in a relatively low bioavailability (50–60%).[22] In addition, metformin HCl has a very short half-life (2–4 h); therefore, frequent drug dosing are necessary for effective therapy. Furthermore, metformin HCl treatment could increase the incidence of gastrointestinal symptoms such as increased flatulence, abdominal pain, anorexia, cramps, nausea, vomiting, diarrhea and weight loss, which collectively result in patient non-compliance.[23,24] The development of a sustained release formulation of metformin HCl might represent a solution for the abovementioned drawbacks *via* improving gastrointestinal tolerability, allowing once-daily dosing and thereby enhancing patient compliance.

In the current study, therefore, we aimed at developing a novel pH-sensitive formulation based on poly(methyl methacrylate)-*grafted*-ghatti gum copolymer (GG-*g*-PMMA), which could help improve the bioavailability of drug product, reduce the dosing frequency and decrease the gastrointestinal toxicity.

2. Materials and methods

2.1. Materials

Metformin hydrochloride was provided as a gift from Salius Pharma, Mumbai, India. Ghatti gum (GG) was purchased from Sigma-Aldrich, MO, USA. Ceric ammonium nitrate (CAN) was purchased from the Merck Specialties Pvt. Ltd., Mumbai, India. Methyl methacrylate (MMA) was procured from Rankem India Pvt. Ltd., Mumbai, India. Chitosan (CAS Number 9012-76-4, 50 000–190 000 Da, 75–85% deacetylated) was purchased from Merk Ltd., Mumbai, India. Hypromellose (CAS 9004-65-3, HPMC E 15 LV Premium, apparent viscosity 12–18 cps), microcrystalline cellulose (MCC; CAS 9004-34-6; Avicel® PH-101; ~50 μm particle size), and talc were procured from the Merk Ltd., Mumbai, India. All other solvents, reagents and chemicals used were of analytical grade.

2.2. Synthesis of poly(methyl methacrylate)-*grafted*-ghatti gum (GG-*g*-PMMA)

Free radical polymerization reaction was adopted to synthesize GG-*g*-PMMA using various ratios of ghatti gum (GG) : methyl methacrylate (MMA) and different amounts of ceric ammonium nitrate (CAN; a redox initiator)[25] (Table 1). Briefly, accurately weighed 1 g of GG was dispersed in 50 ml of double distilled water and heated for 30 min. To initiate polymerization reaction, definite quantities of MMA and CAN were added to GG aqueous solution and polymerization reaction was continued at 80 °C for 1 h. The resultant solution was cooled to room temperature and then poured into excess of methanol and kept overnight. The resultant copolymer was filtered, rinsed with methanol, and finally dried at 55 °C in a hot air oven for 12 h. The obtained GG-*g*-PMMA copolymer was subjected to alkaline hydrolysis using 1 M NaOH solution with stirring for 1 h at 75 °C. The hydrolyzed copolymer was then collected *via* filtration, rinsed with methanol repeatedly, and dried in a hot air oven at 55 °C overnight. The percent grafting (% G) and percent grafting efficiency (% GE) were calculated using the following equations.[25,26]

$$\% \text{ Grafting } (\% \ G) =$$

$$\frac{\text{weight of graft copolymer} - \text{weight of native gum}}{\text{weight of native gum}} \times 100$$

$$\% \text{ Grafting efficiency } (\% \ GE) =$$

$$\frac{\text{weight of graft copolymer} - \text{weight of native gum}}{\text{weight of monomer}} \times 100$$

2.3. Characterization of ghatti gum grafted copolymer

2.3.1. Elemental analysis. Elemental analysis of GG, MMA, and GG-*g*-PMMA was performed using FlashSmart™ elemental analyzer (Thermo Fisher Scientifics, MA, USA) for estimating hydrogen, carbon and nitrogen content.

Table 1 Synthetic details of polymethyl methacrylate-*grafted*-ghatti gum (GG-*g*-PMMA)[a]

Batch	GG (g)	CAN (mg)	MMA (g)	G (%)	GE (%)
G1	1	100	2	12.3 ± 1.1	6.15 ± 0.52
G2	1	100	6	31.4 ± 2.5	5.23 ± 0.36
G3	1	100	10	51.2 ± 2.3	5.12 ± 0.41
G4	1	100	14	41.2 ± 1.9	2.94 ± 0.32
G5	1	200	2	13.3 ± 1.2	6.65 ± 0.78
G6	1	200	6	39.9 ± 2.8	6.65 ± 0.77
G7	1	200	10	62.6 ± 2.2	6.26 ± 0.63
G8	1	200	14	43.4 ± 1.8	3.1 ± 0.41
G9	1	300	2	16.1 ± 0.9	8.05 ± 0.54
G10	1	300	6	91.6 ± 3.3	15.26 ± 0.82
G11	1	300	10	77.3 ± 2.6	7.73 ± 0.63
G12	1	300	14	60.9 ± 1.7	4.35 ± 0.37
G13	1	400	2	15.8 ± 0.8	7.9 ± 0.61
G14	1	400	6	45.5 ± 2.3	7.5 ± 0.54
G15	1	400	10	63.3 ± 3.5	6.3 ± 0.43
G16	1	400	14	51.2 ± 2.8	3.65 ± 0.21

[a] Data represents mean ± SD where $n = 3$.

2.3.2. Proton nuclear magnetic resonance analysis (^{1}H-NMR).

Structural characterization of GG-*g*-PMMA was conducting using ^{1}H-NMR spectroscopy. The native gum was dissolved in deuterium oxide (D_2O), while the graft copolymer (GG-*g*-PMMA) was dissolved in dimethyl sulfoxide (DMSO). The NMR spectra of GG and GG-*g*-PMMA were taken using Agilent NMR spectrophotometer (Santa Clara, CA, USA) at 400 MHz at room temperature.

2.3.3. Scanning electron microscopy (SEM).

The morphology of the samples was observed using EVO LS scanning electron microscope (Smart SEM, Zeiss EVO LS, Frankfurt, Germany). The samples were coated by gold to improve electron beams conductivity and SEM images were obtained at an accelerating voltage of 15 kV with a working distance of 10 mm and an energy dispersive X-ray (EDX) detector.[27]

2.3.4. Acute oral toxicity.

The acute oral toxicity test was conducted according to the guidelines of the Organization for Economic Cooperation and Development. Briefly, six nulliparous and non-pregnant female albino mice were randomly selected for acute oral toxicity study. Animals were kept under standard conditions of temperature (25 ± 1 °C) and relative humidity (60 ± 10%), and had free access to water and standard chow diet. One animal was randomly chosen and was kept as a control without any treatment. A single dose of GG-*g*-PMMA (2000 mg kg^{-1}) was orally administered *via* an oral gavage to a single female mice and the animal was examined cautiously for the first 30 minutes, then for 4 hours. After the survival of a handled mouse, 4 additional mice were treated with the same dose under similar conditions. The animals were closely monitored for any toxic effect during the first 4 h and then at daily intervals for a period of 14 days for any toxic effect. Mortality was detected by visual observation.[28,29]

2.3.5. Histopathological examination.

The liver, kidney, lung, brain and heart from one mouse that survived the toxicity test, were fixed in 10% buffered formalin for 24 h. The dissected tissues were subjected to dehydration in a graded series of 50, 70 and 100% ethyl alcohol. The tissues were embedded in paraffin blocks and sectioned at approximately 5–7 μm thickness and were then stained with hematoxylin and eosin (H&E). Stained sections were examined adopting bright field contrast enhancing approach using a light microscope (Motic, B1 series System Microscope, India) fitted with camera (Magnus, MITS, India) at ×40 magnification.

2.4. Preparation of metformin HCl pellets

The composition of metformin HCl pellet formulations was summarized in Table 2. A matrix pellet formulations consisting of metformin HCl, GG-*g*-PMMA, hypromellose (binder), microcrystalline cellulose (pelletization aid), and talc (glidant/lubricant) were prepared by extrusion/spheronization. Briefly, drug, GG-*g*-PMMA and other excipients were mixed together at room temperature for 15 min. Then a mixture of water-: isopropyl alcohol (H_2O : IPA) was added slowly to agglomerate the powder mixture into a wet mass. The wet mass was then processed in a rotating roller extruder (EXT 65/037, R. R. Enterprises, India). The collected extrudates were transferred into a spheronizer (SPH 150/010, R. R. Enterprises, India) and were spheronized for 10 min at a spheronization speed of 1600 rpm. The resulting pellets were collected and were dried overnight at 40 °C in a hot air oven. In order to prevent pellet aggregation, surface erosion and burst drug release in the stomach, the resulting drug loaded pellets were eventually film-coated with chitosan (50 000–190 000 Da, 75–85% deacetylated). Chitosan was selected as a coating polymer considering its resistance to be digested by digestive enzymes in the upper gastrointestinal tract,[30,31] however, being hydrolyzed by microbial enzymes inside the colon.[32] Pellets were film coated using a fluidized bed coater (Jiangsu Jiafa granulating drying

Table 2 Formulation chart for metformin HCl-loaded pellets prepared by using GG-*g*-PMMA

Batch	Metformin HCl (mg)	MCC (mg)	Hypromellose (mg)	Talc (mg)	GG-*g*-PMMA (mg)	H$_2$O : IPA (5 : 3)	Total (mg)
F1	500	550	40	50	10	0.8	1150
F2	500	540	40	50	20	0.8	1150
F3	500	530	40	50	30	0.8	1150
F4	500	520	40	50	40	0.8	1150
F5	500	510	40	50	50	0.8	1150
F6	500	500	40	50	60	0.8	1150

equipment, Changzhou, China) with spraying rate of 1 g min^{-1}, inlet temperature of 55 °C and atomizing pressure of 0.8–1.0 bars.[33]

2.5. Characterization of metformin HCl pellets

2.5.1. Fourier transform infrared spectroscopy (FTIR). FTIR spectroscopy was utilized to assess drug–polymer interactions. FTIR spectra of pure drug, GG, GG-*g*-PMMA, physical mixture of pure drug + GG-*g*-PMMA, and metformin loaded GG-*g*-PMMA pellets were recorded using FTIR spectrometer (8400S, Shimadzu, Japan). The sample to be analyzed was compressed with KBr into a thin film pellet. The scanning range was 500–4000 cm^{-1}.[34]

2.5.2. Differential scanning calorimetry (DSC). DSC studies for pure drug, GG, GG-*g*-PMMA, physical mixture of pure drug + GG-*g*-PMMA, and metformin loaded GG-*g*-PMMA pellets was conducted using differential scanning calorimeter (DSC-60, Shimadzu, Japan).[35] DSC thermograms were recorded in the temperature range of 20–350 °C, at a heating rate of 10 °C min^{-1}.

2.5.3. X-ray diffraction (XRD). XRD of pure drug, GG, GG-*g*-PMMA, physical mixture of pure drug + GG-*g*-PMMA, and metformin loaded GG-*g*-PMMA pellets was conducted using Benchtop Advance X-ray powder diffractometer (Bruker AXS GmbH, Karlsruhe, Germany).

2.6. Evaluation of prepared pellets

2.6.1. Particle size. Particle size of metformin HCl pellets was determined using polarized light microscopy (Zeiss, Me 63C, Frankfurt, Germany) fitted with a calibrated ocular micrometer.[36]

2.6.2. Microscopic analysis. Microscopic photographs of prepared metformin HCl pellets were taken at 100× magnification by EVO LS scanning electron microscope (Smart SEM, Zeiss EVO LS, Frankfurt, Germany) at room temperature. For this analysis, samples were coated by gold for enhancing electron beams conductivity and an accelerating voltage of 5.0 kV with a working distance of 10 mm in line with energy dispersive X-ray (EDX) detector was implied. Microscopic photographs obtained were observed to analyze the shape of metformin HCl pellets.[37]

2.6.3. Determination of drug loading and drug entrapment efficiency. 50 mg of drug loaded pellets were grounded and kept suspended in 100 ml phosphate buffer saline (pH 6.8) at room temperature for 24 h with constant agitation. The drug solution was filtered and the drug content was analyzed spectrophotometrically at λ_{max} of 232 nm. Drug loading and entrapment efficiency were determined using the following equations:

$$\text{Drug loading } (\%) = \frac{\text{weight of drug in pellets}}{\text{weight of pellets}} \times 100$$

$$\text{Drug entrapment } (\%) = \frac{\text{actual drug loading}}{\text{theoretical drug loading}} \times 100$$

2.6.4. Micromeritic studies. The Carr's compressibility index and the Hausner's ratio were determined to provide an insight onto the flow properties. The Hausner's ratio and Carr's index were determined as follows:

$$\text{Carr's index} = \frac{\text{tapped density} - \text{bulk density}}{\text{tapped density}} \times 100$$

$$\text{Hausner's ratio} = \frac{\text{tapped density}}{\text{bulk density}}$$

Angle of repose method[34] was also conducted by pouring pellets through a funnel on the horizontal surface. The height and the diameter of powder cone formed upon passage of the pellets through the funnel were measured. The angle of repose was then determined using the following equation:

$$\text{Angle of repose } (\theta) = \tan^{-1}\frac{\text{height of powder cone}}{\text{radius of powder cone}}$$

2.7. *In vitro* drug release and release kinetics

The *in vitro* release of metformin HCl from optimized GG-*g*-PMMA-based formulation was conducted using USP Type-II apparatus (Electrolab, Mumbai, India) assembled with paddles. Briefly, definite weight of pellets (equivalent to 500 mg of metformin HCl) were filled in size 00 hard gelatin capsules. Dissolution study was conducted at gastric pH (0.1 N HCl; pH 1.2) and intestinal pH (PBS; pH 6.8) for 2 and 10 h, respectively, at 37 ± 0.5 °C and paddle speed was set at 50 rpm. At definite time intervals (0.5, 1, 2, 3, 4, 6, 8, 10 and 12 h), 3 ml aliquot samples were withdrawn from the dissolution medium and replaced with an equal volume of fresh medium to maintain sink conditions. The drug concentration in each sample was quantified spectrophotometrically at λ_{max} of 232 nm. Drug release data was fitted in different kinetic models to determine the release kinetics.

2.8. *In vivo* antidiabetic activity

For induction of diabetes, Wistar albino rats (male; weighing 250–300 g) were intraperitoneally (i.p.) treated with a single dose of nicotinamide in physiological saline (110 mg kg^{-1}) followed by an i.p. injection of streptozotocin (STZ; 60 mg kg^{-1}) 15 min later. At 4 days post nicotinamide–STZ treatment, blood glucose levels were determined to assess the extent of diabetes induction. Rats with a basal blood glucose level above 200 mg dl^{-1} were considered diabetic.[38] To assess the hypoglycemic activity of different formulations, rats were randomly categorized into four groups ($n = 6$); one non-diabetic control group and three diabetic groups. The non-diabetic control group was orally treated with sodium carboxymethyl cellulose (sodium CMC; 0.5% w/v) and served as negative controls. The other three diabetic groups were treated with sodium CMC (positive control), marketed formulation (Glycomet® SR 500 mg tablet) in sodium CMC solution at a dose of 500 mg kg^{-1} (diabetic

standard), and optimized formula of GG-*g*-PMMA metformin pellets in sodium CMC solution at a dose of 500 mg kg^{-1} (diabetic test), respectively. Food was withdrawn from the rats 12 h before drug administration. All rats had free access to water throughout the study. The study protocol was approved by the Ethical Committee of JSS College of Pharmacy, Mysuru, India (CPCSEA Approval No. P17248/2017). At predetermined time points post drug administration (0, 2, 4, 6, 8, 10 and 12 h), blood samples were withdrawn from the retro-orbital plexus of each rat and blood glucose levels were measured using glucometer (an Accu-Check® Roche Diagnostic Corporation, USA). 14 days later, blood samples were collected and centrifuged at 3000 rpm for 15 min. The obtained serum samples were assayed for the following parameters: total cholesterol, triglyceride, and total protein levels.

2.9. Statistical analysis

All values are expressed as the mean ± SD. Statistical analysis was performed using ANOVA test (SPSS software version 16; SPSS Inc., Chicago, USA). The level of significance was set at $p < 0.05$.

3. Results and discussion

3.1. Synthesis of polymethylmethacrylate-*grafted*-ghatti gum (GG-*g*-PMMA)

Various grades of the graft copolymer were synthesized by varying methyl methacrylate (MMA; monomer) and ceric ammonium nitrate (CAN) concentrations (Table 1). Synthesis of GG-*g*-PMMA was conducted *via* free radical polymerization reaction using CAN as reaction initiator.[25] CAN is an electron deficient molecules; it can attract electrons from alcoholic oxygen in ghatti gum (GG) to form a new Ce–O bond. This Ce–O bond is more polar than O–H bond and, thereby, is easily cleaved to form free radical site on GG backbone. The resulting free radicals on GG backbone initiate the graft copolymerization of MMA onto GG backbone *via* covalent coupling of GG free radicals with MMA monomer units, resulting into chain propagation with subsequent production of polymethyl methacrylate graft chains.[28,29]

3.2. Effect of polymerization parameters on GG-*g*-PMMA synthesis

3.2.1. Effect of monomer (MMA) concentration on grafting.
The impact of monomer concentration on both percentage grafting (% *G*) and percentage grafting efficiency (% GE) was investigated. As shown in Table 1, % *G* was found to be increased with increase in monomer concentration up to GG : monomer ratio of 1 : 10. This can be ascribed to the fact that as the concentration of monomers (MMA) increases, more and more of the monomers become available for attachment to the initiated backbone, which in turn, resulted in a steady increase in percentage grafting. Nevertheless, raising the monomer concentration behind such ratio was found to compromise grafting percentage. This might be attributed to the higher solution viscosity at higher monomer concentration,

which in turn, might hinder the diffusion of monomers from bulk solution to GG surface, resulting in a decrease in percentage grafting. These findings are in agreement with those of Gowrav *et al.*[39] By contrary, with the exception of G10, percentage grafting efficiency (% GE) remarkably decreased with increase in monomer concentration. Such finding might be attributed to the possible steric hindrance encountered by the grafted chains, which may act as diffusion barriers against the efficient diffusion of monomer to the polymer backbone.[40,41]

3.2.2. Effect of initiator concentration on grafting.
To study the effect of initiator concentration, the concentration of CAN was changed from 100 to 400 mg, and its effect on the grafting was investigated. As shown in Table 1, both % *G* and % GE were increased significantly by increasing CAN concentrations up to 300 mg and then decreased upon further increase in initiator concentration. With increasing CAN concentration, the active sites on the GG backbone increase, which results in an increase in both the percentage grafting and percentage grafting efficiency. However, at higher CAN concentration (>300 mg), the extra free radicals remain in the polymerization medium and therefore the monomers get polymerized, which result in increase in the homopolymerization concentration. In addition, excessive radical concentration present in polymerization medium might also enhance the termination rate of the growing grafted chains resulting in lower grafting.[41,42]

3.3. Selection of optimized graft copolymer (GG-*g*-PMMA)

The optimized graft copolymer (GG-*g*-PMMA) was selected on the basis of higher percentage grafting and efficiency. From Table 1, it was evident that G10 formula, obtained at a monomer (MMA) concentration of 6 g and an initiator (CAN) concentration of 0.3 g, exhibited highest percentage grafting (% *G* of 91.6 ± 3.3) and superior percentage grafting efficiency (% GE of 15.26 ± 0.82). Consequently, G10 formula was selected as an optimized formula and was subjected for further investigations.

3.4. Characterization of optimized GG-*g*-PMMA

3.4.1. Elemental analysis.
In order to assess the efficacy of grafting reaction, elemental analysis study was conducted. The results of elemental analysis of GG and optimized graft copolymer (G10) are summarized in Table 3. A remarkably higher percentage of hydrogen and carbon was observed in the grafted copolymer (G10), compared to the native GG, indicating successful grafting of MMA monomers onto the GG backbone.

3.4.2. Proton nuclear magnetic resonance analysis (^{1}H-NMR).
To further confirm the efficient grafting of MMA on the GG backbone, ^{1}H-NMR spectra of both grafted copolymer (GG-*g*-

Table 3 Elemental analysis of optimized GG-*g*-PMMA

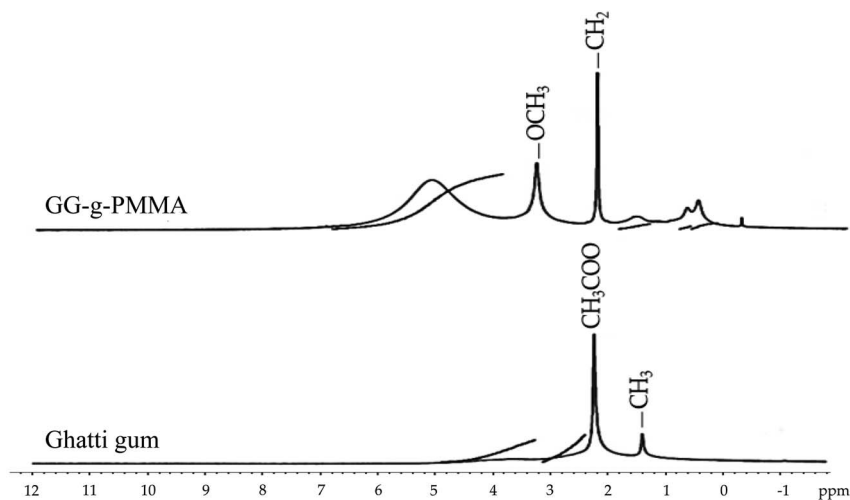| Polymer	% C	% H	% N
GG	38.24	6.43	0.00
MMA	60.04	8.01	0.00
GG-*g*-PMMA	42.47	6.71	0.00

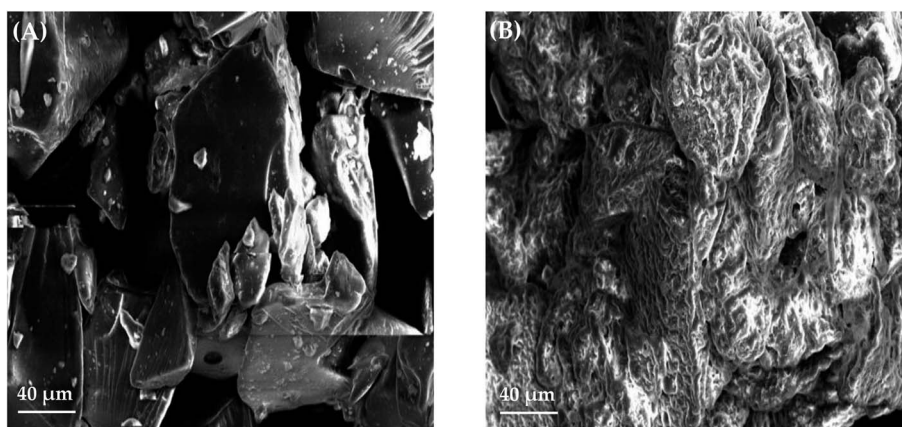**Fig. 1** ^{1}H-NMR spectra of purified ghatti gum (GG) and ghatti gum grafted copolymer (GG-*g*-PMMA).

Fig. 2 SEM images of (A) purified ghatti gum (GG) and (B) ghatti gum grafted copolymer (GG-*g*-PMMA) at magnification 1000×.

PMMA) and purified GG were recorded and analyzed (Fig. 1). ^{1}H-NMR spectrum of GG shows a characteristic peaks at 1.3 δ and 2.2 δ, corresponding to the protons of –CH$_3$ and CH$_3$COO groups of GG, respectively. The ^{1}H-NMR spectrum of GG-*g*-PMMA shows distinct peaks of –CH$_2$ and –OCH$_3$ of MMA appeared at 2.47 δ, and 3.52 δ, respectively. ^{1}H-NMR spectroscopy results were consistent with elemental analysis findings, verifying the efficient grafting of MMA on GG.

3.4.3. Scanning electron microscopy (SEM). SEM analysis of GG (Fig. 2A) and its grafted copolymer GG-*g*-PMMA (Fig. 2B) evidently reflect morphological changes from flaky structure of GG to porous spongy structure, presumably, due to the grafting of GG backbone by PMMA chains.

3.5. Acute oral toxicity

To assess the oral toxicity of grafted copolymer, non pregnant nulliparous female mice were orally administered a single dose of GG-*g*-PMMA (2000 mg kg^{-1}) and the animals were observed for mortality. No mortalities were observed among tested animals up to 14 days post grafted copolymer administration.

Furthermore, the LD$_{50}$ of GG-*g*-PMMA was found to be greater than 2000 mg kg^{-1}, consequently, GG-*g*-PMMA can be classified under category 5 "with zero toxicity rating" according to Globally Harmonized System of Classification and Labelling of Chemicals (GHS).[25,28]

3.6. Histopathological analysis

Histological examination of liver tissues in both control and test animals showed normal hepatocytes, Kupffer cells and large polygonal cells (Fig. 3A). Light microscopy examination of kidney tissues demonstrated similar morphology for the cuboidal epithelial cells of loop of Henle and collecting tubules (Fig. 3B). Micrograph of heart tissue of both control and test animals showed homogenous cardiomyocytes connected by intercalated discs (Fig. 3C). Histological examination of lung tissues of both control and test animals showed no sign of morphological changes (Fig. 3D). Finally, brain tissue showed similar granular cells morphology in both control and test animals (Fig. 3E).
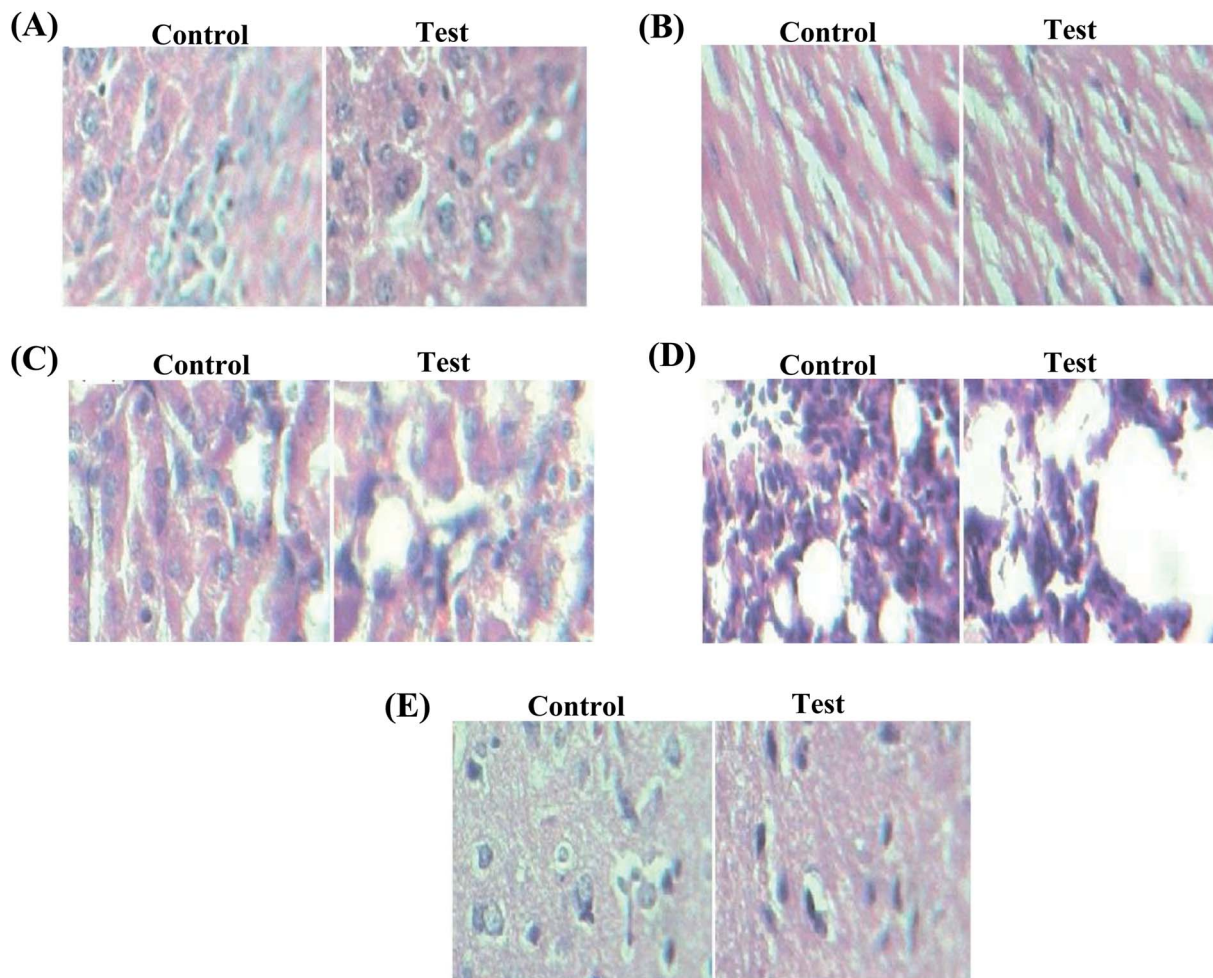
Fig. 3 Histological micrographs of (A) liver, (B) kidney, (C) heart, (D) lung and (E) brain of mice upon treatment with GG-*g*-PMMA (magnification 40×).

3.7. Preparation of metformin HCl-loaded pellets

A matrix pellet formulations consisting of metformin HCl, GG-*g*-PMMA, hypromellose (binder), microcrystalline cellulose (pelletization aid), and talc (glidant/lubricant) were prepared by extrusion/spheronization.[43,44]

3.7.1. Characterization of metformin HCl-loaded pellets

3.7.1.1. Surface morphology and particle size analysis of metformin HCl pellets. The surface morphology and shape of metformin HCl pellets were inspected under scanning electron microscopy (SEM). SEM analysis showed that the prepared pellets have a spheroidal shape with smooth surfaces (Fig. 4). Particle size analysis of different batches was performed using polarized light microscopy fitted with a calibrated ocular micrometer. All pellet batches showed a narrow particle size distribution ranging from 1178 ± 166 to 1386 ± 157 μm.

3.7.1.2. Micromeritic properties. Good flow properties play an important role in further processing of pellets such as filling in capsules or compressing into tablets. In this study, flow properties of different pellet batches were evaluated in terms of Carr's index, Hausner's ratio and angle of repose (Table 4). It was evident that all batches showed good flow properties.

Furthermore, no significant differences in the evaluated parameters were observed within the different batches.

3.7.1.3. Drug loading and entrapment efficiency. Drug loading and entrapment efficiency of pellets are reported in Table 4.
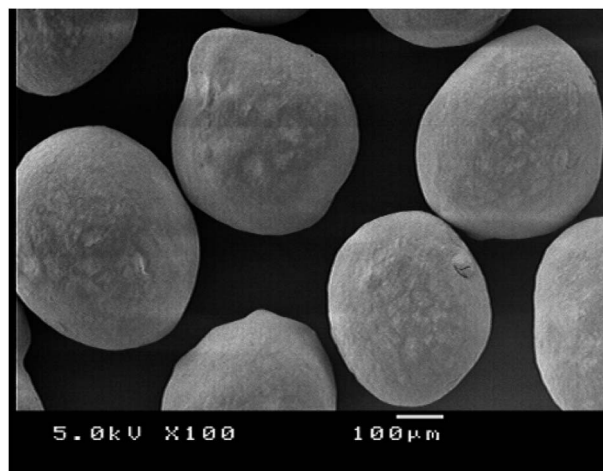

Fig. 4 Microscopic photograph of metformin HCl pellets prepared by using GG-*g*-PMMA.

Table 4 Characterization parameters of GG-g-PMMA-based metformin HCl pellets[a]

Batch	Angle of repose (°)	Carr's index (%)	Hausner's ratio	Particle size (μm)	Drug loading (%)	Entrapment efficiency (%)
F1	22.69 ± 0.63	9.87 ± 0.23	1.11 ± 0.16	1269 ± 129	54.47 ± 0.48	91.25 ± 0.52
F2	21.53 ± 0.39	7.96 ± 0.73	1.09 ± 0.02	1195 ± 142	52.14 ± 0.11	89.53 ± 0.32
F3	23.34 ± 0.44	8.12 ± 0.39	1.08 ± 0.19	1386 ± 157	57.64 ± 0.74	94.97 ± 0.53
F4	25.41 ± 0.09	8.73 ± 0.18	1.10 ± 0.29	1253 ± 114	53.89 ± 0.29	87.32 ± 1.12
F5	25.83 ± 0.72	8.92 ± 0.47	1.10 ± 0.02	1217 ± 173	54.31 ± 0.46	90.74 ± 0.19
F6	26.37 ± 0.35	9.57 ± 0.59	1.11 ± 0.14	1178 ± 166	55.72 ± 0.63	88.63 ± 0.44

[a] Data represent mean ± SD where $n = 3$.

Percentage drug loading for different metformin HCl pellet formulations was in the range of 52.14 ± 0.11% to 57.64 ± 0.74%, while entrapment efficiency percentage ranged from 87.32 ± 1.12 to 94.97 ± 0.53. The drug loading and entrapment efficiency of batch F3 was noted to be higher than those of other batches (57.64 ± 0.74% and 94.97 ± 0.53%, respectively). Consequently, batch F3 was selected for further investigations.

3.8. Drug–polymer interaction studies

3.8.1. Fourier transform infrared spectroscopy (FTIR). FTIR spectra of pure drug, grafted copolymer (GG-g-PMMA), physical mixture and optimized pellet formulation are depicted in Fig. 5. FTIR spectra of metformin HCl (Fig. 5A) shows the existence of characteristic absorption peaks at 3372 cm^{-1} for N–H (stretching), 2800–3050 cm^{-1} for CH$_3$ (aliphatic, stretching), 1584 cm^{-1} for C=N (stretching), and 1477 cm^{-1} for N–H (bending). The spectrum of GG-g-PMMA (Fig. 5B) showed characteristic peaks at 3443 cm^{-1} for O–H (stretching), 1667 cm^{-1} for C=O (stretching), and 1032 cm^{-1} for C–O (stretching). Of interest, the characteristic absorption peaks of both metformin HCl and grafted copolymer (GG-g-PMMA) were retained in the FTIR spectra of both physical mixture (Fig. 5C)

and optimized pellet formulation (Fig. 5D) without the disappearance of existing peaks or the appearance of new peaks. These results suggest the absence of any pronounced interaction and/or incompatibilities between the drug and the graft copolymer.

3.8.2. Differential scanning calorimetry (DSC). To confirm the compatibility of metformin HCl and graft copolymer (GG-g-PMMA), DSC studies were conducted. DSC thermograms of pure drug, GG-g-PMMA, physical mixture, and prepared formulation are represented in Fig. 6. The thermogram of metformin HCl showed a sharp endothermic peak at 230.86 °C corresponding to the melting point of the pure drug in the crystalline form (Fig. 6A). The thermogram of GG-g-PMMA showed an endothermic peak at 116.83 °C (Fig. 6B). Of interest, no shift in the endothermic peak of metformin HCl was observed in either the physical mixture (Fig. 6C) or the optimized pellet formulation (Fig. 6D). This suggested the absence of any change in drug crystallinity, confirming drug–polymer compatibility.

3.8.3. X-ray diffraction (XRD). Powder X-ray diffraction (XRD) analysis was performed to address any possible changes
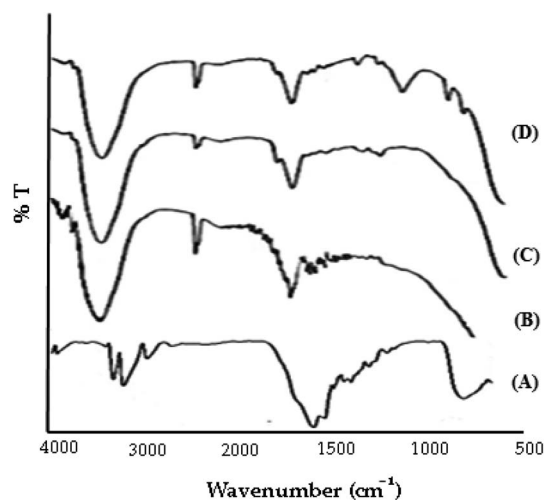
Fig. 5 Fourier transform infrared spectra of (A) metformin HCl, (B) GG-g-PMMA copolymer, (C) physical mixture of metformin HCl and GG-g-PMMA copolymer and (D) optimized metformin HCl pellet formulation.
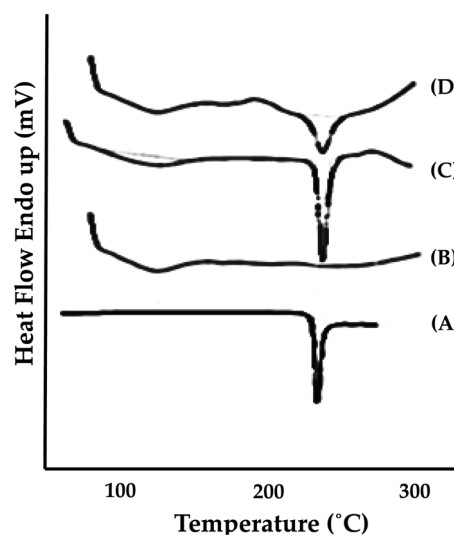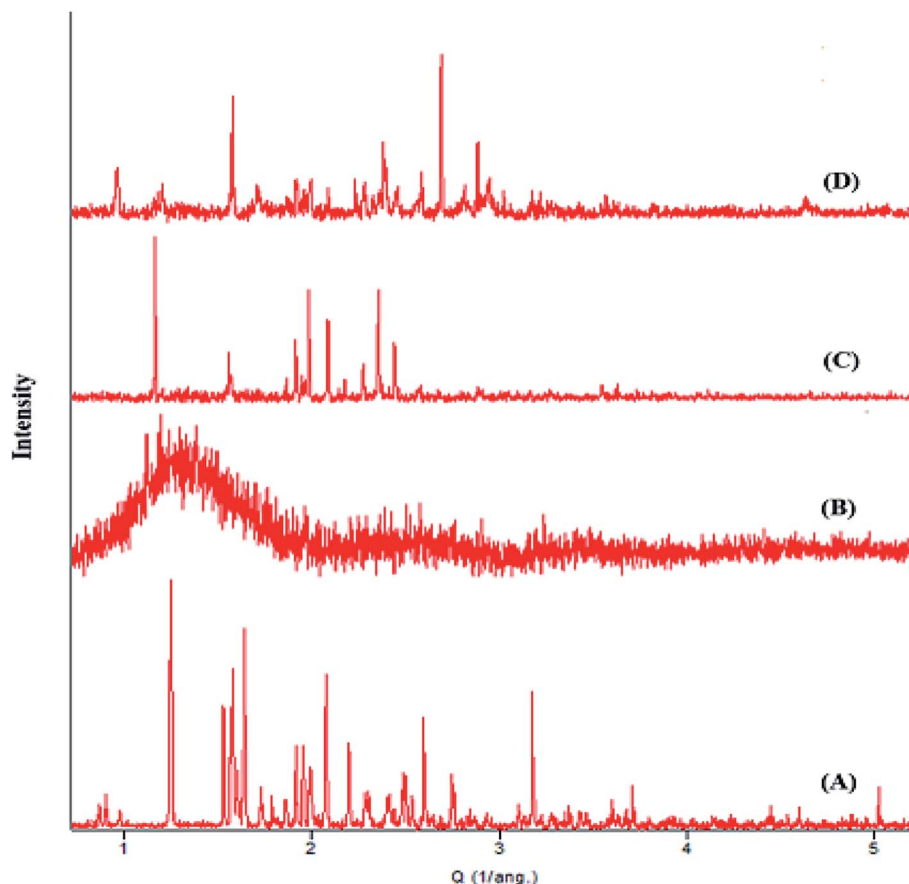
Fig. 6 Differential scanning calorimetry thermograms of (A) metformin HCl, (B) GG-g-PMMA copolymer, (C) physical mixture of metformin HCl and GG-g-PMMA copolymer and (D) optimized metformin HCl pellet formulation.

Fig. 7 Powder XRD diffractogram of (A) metformin HCl, (B) GG-*g*-PMMA, (C) physical mixture of metformin HCl and GG-*g*-PMMA copolymer and (D) optimized metformin HCl pellet formulation.

in the crystallinity due to drug–polymer interaction. The X-ray diffractogram of pure drug, GG-*g*-PMMA, physical mixture and optimized pellet formulation are depicted in Fig. 7. The PXRD spectrum of pure metformin HCl showed sharp crystalline peaks, indicating the crystallinity of the drug (Fig. 7A). On the other hand, the XRD spectrum of grafted copolymer (GG-*g*-PMMA) showed broad bands located at low diffraction angle (2θ) values, demonstrating the amorphous nature of the graft copolymer (Fig. 7B). Of interest, X-ray diffractogram of physical mixture (Fig. 7C) and optimized pellet formulation (Fig. 7D) suggest that the drug retained its crystalline nature as indicated by the presence of several sharp peaks with less noise. In addition, intensities at the different 2θ values for metformin HCl were maintained in the optimized pellet formulation, indicating the compatibility between the drug and formulation components.

3.9. *In vitro* drug release and release kinetics

The *in vitro* release of metformin HCl from the optimized pellet formulation was carried out using buffer change method to mimic the gastrointestinal tract (GIT) environment. As shown in Fig. 8, negligible drug release was observed at the initial 2 h in 0.1 N HCl solution (pH 1.2), where only 2.07 $\pm$ 1.55% of the loaded drug was release at the end of 2 h. On the other hand, the

drug was readily released at higher pH (pH 6.8); with up to 93.86 $\pm$ 2.16% of the loaded drug was released at the end of 12 h. The pH-dependent release of metformin HCl from GG-*g*-PMMA based matrix pellets might be ascribed to the fact that, at acidic pH, the carboxyl groups of graft copolymer (GG-*g*-PMMA), used
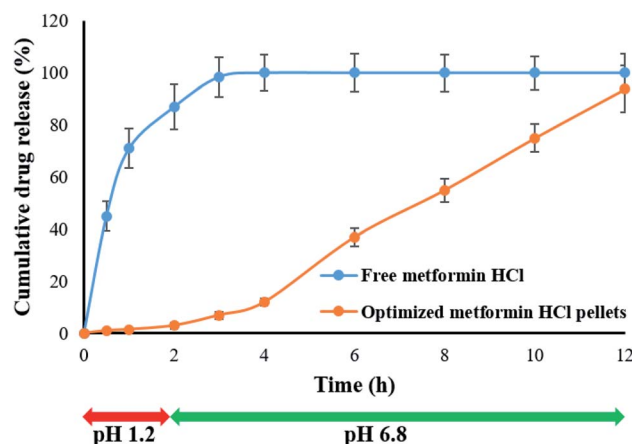

Fig. 8 *In vitro* release profiles of plain metformin HCl and optimized metformin HCl pellets prepared using GG-*g*-PMMA and in pH 1.2 and pH 6.8 buffer media.
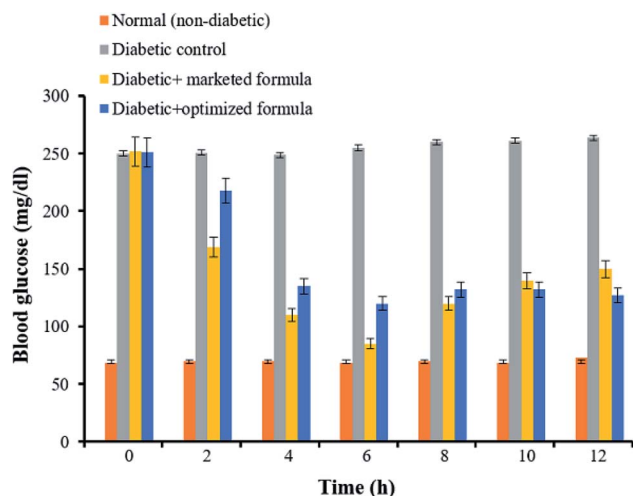
Fig. 9 Blood glucose levels in nicotinamide–STZ induced diabetic rats treated with marketed formulation and optimized metformin HCl formulation.

3.10. *In vivo* antidiabetic activity

Administration of both nicotinamide (NA) and streptozotocin (STZ) has been adopted to induce experimental diabetes in the rats. It is well recognized that STZ does damage to pancreatic B-cells, while NA is given to rats to partially protect insulin-secreting cells against STZ.[47] The induction of diabetes in experimental rats was assessed 2–4 days post NA/STZ treatment *via* measuring blood glucose levels in rats. Rats with a basal blood glucose level above 200 mg dl^{-1} were considered diabetic.[38] In this study, the hypoglycemic activity of an optimized GG-*g*-PMMA-based metformin HCl pellet formulation was evaluated in rats with streptozotocin-induced diabetes, and compared with that of a marketed formulation (Glycomet® SR 500 mg tablet). As shown in Fig. 9, treatment with NA and STZ efficiently induced diabetes in rats. The blood glucose levels in diabetic control group were significantly higher than that in non-diabetic control group (249.87 ± 3.82 mg dl^{-1} to 263.74 ± 2.5 mg dl^{-1} *vs.* 68.48 ± 2.84 mg dl^{-1} to 72.52 ± 3.2 mg dl^{-1}, respectively). Rats treated with either a marketed formulation (diabetic standard group) or optimized metformin HCl formulation (diabetic test group) showed a significant decrease in blood glucose levels, compared to diabetic control group. Of interest, the blood glucose lowering activity of optimized metformin HCl formulation was sustained for a prolonged period of time (up to 12 h post administration), compared to marketed formulation. These results confirm the potent hypoglycemic efficacy of the optimized metformin HCl formulation.

It is worth noting that diabetes is associated with various metabolic deviations in animals such as changes in lipid profile and protein content.[48] Accordingly, various biochemical parameters such as total cholesterol, triglyceride, and total protein levels were estimated following treatment with optimized metformin formulation. As depicted in Table 5, diabetes induction causes a significant increase in total cholesterol and triglycerides levels and decrease total protein levels, which was accompanied with a significant reduction in body weight. On the other hand, treatment with either a marketed formulation or optimized metformin HCl formulation was able to correct the metabolic disturbances observed in diabetic control group. The biochemical parameter values obtained for the marketed formulation as well as the optimized formulation were comparable to those observed with non-diabetic control group.

for the formulation of pellets, remain unionized and favor the formation of hydrogen bonding between carboxyl groups of GG-*g*-PMMA in acidic solution. This makes the polymer segments rigid, which in turn, hampers water absorption, minimizes swelling and hinders drug release. On the other hand, at alkaline pH, carboxyl groups of GG-*g*-PMMA become ionized, and thereby, increase the repulsion between resultant carboxylate ions (COO$^-$), resulting in relaxation of copolymer chains with subsequent pellet swelling and remarkable drug release.[45,46] The fractions of glucuronic acid, galacturonic acid and uronic acid present in pristine GG contribute towards carboxyl groups in grafted copolymer. Nonetheless, the methyl ester of methacrylic acid (MMA) also gets ionized at basic pH to give more carboxylate ions (COO$^-$); augmenting pH sensitivity of grafted copolymer. Similar findings were reported by Gowrav *et al.* who demonstrated that the hypoglycemic agent, glimepiride, showed a pH dependent release from pellets formulated with the pH-sensitive polacrylamide grafted guar gum copolymer.[39]

To address the mechanism of metformin HCl release from the prepared drug-loaded pellets, the obtained *in vitro* release data were fitted to different kinetic models.[36] From the kinetic modeling data, drug release from pellet formulation was found to follow Korsmeyer–Peppas model with r^2 value 0.980. This suggests that drug release from pellets is mainly driven by Fickian diffusion and/or polymeric matrix erosion.

4. Conclusions

In this study, a novel poly(methyl methacrylate)-*grafted*-ghatti gum (GG-*g*-PMMA) copolymer was fabricated and challenged

Table 5 Biochemical parameters and body weight in nicotinamide–STZ induced diabetic rats 14 days post-treatment with marketed formulation and optimized metformin HCl formulation

Group(s)	Cholesterol (mg dl^{-1})	Triglyceride (mg dl^{-1})	Total protein (g dl^{-1})	Change in body weight (g)
Non-diabetic control	112.28 ± 3.96	81.44 ± 2.05	7.84 ± 0.64	+20.84
Diabetic control	145.62 ± 3.02	106.7 ± 3.62	4.37 ± 0.43	−33.71
Diabetic + marketed formula	107.92 ± 5.23	83.79 ± 0.05	6.78 ± 0.49	+28.15
Diabetic + optimized formula	116.27 ± 4.59	86.93 ± 1.03	5.12 ± 0.57	+9.97

for its efficacy as a pH sensitive drug delivery system for anti-diabetic therapy. GG-*g*-PMMA copolymer was produced by free radical polymerization technique using ceric ammonium nitrate as a redox initiator. The fabricated graft copolymer was characterized chemically, morphologically and biologically. In addition, the optimized graft copolymer was formulated into pellets by extrusion/spheronization technique and was loaded with the hypoglycemic agent, metformin HCl. The prepared metformin HCl pellet formulation showed a pH-dependent sustained drug release. In addition, metformin HCl-loaded pellets have elicited promising hypoglycemic efficacy in streptozotocin-induced diabetic rats. To sum up, the free radical polymerization technique is an effective, reproducible and less time-consuming method for the synthesis of graft copolymers that can be used for the manufacturing of pH-sensitive and/or sustained release drug delivery systems.

Conflicts of interest

The authors declare no conflict of interest.

Acknowledgements

References

1 H. Idrees, S. Z. J. Zaidi, A. Sabir, R. U. Khan, X. Zhang and S. U. Hassan, *Nanomaterials*, 2020, **10**, 1970.

2 S. Raveendran, A. K. Rochani, T. Maekawa and D. S. Kumar, *Materials*, 2017, **10**, 929.

3 R. Song, M. Murphy, C. Li, K. Ting, C. Soo and Z. Zheng, *Drug Des., Dev. Ther.*, 2018, **12**, 3117–3145.

4 R. A. Osmani, E. Singh, K. Jadhav, S. Jadhav and R. Banerjee, *Applications of Advanced Green Materials*, 2021, vol. 1, pp. 573–630.

5 A. M. Wagner, D. S. Spencer and N. A. Peppas, *J. Appl. Polym. Sci.*, 2018, **135**, 46154.

6 A. S. Deshmukh, C. M. Setty, A. M. Badiger and K. S. Muralikrishna, *Carbohydr. Polym.*, 2012, **87**, 980–986.

7 L. Kaur, J. Singh and H. Singh, *J. Food Sci.*, 2009, **74**, E328–E332.

8 H. Sun, L. Yang, M. P. Thompson, S. Schara, W. Cao, W. Choi, Z. Hu, N. Zang, W. Tan and N. C. Gianneschi, *Bioconjugate Chem.*, 2019, **30**, 1889–1904.

9 V. Pillay, A. Seedat, Y. E. Choonara, L. C. du Toit, P. Kumar and V. M. K. Ndesendo, *AAPS PharmSciTech*, 2013, **14**, 692–711.

10 M. Reddy, D. Reddy, A. Moin and H. G. Shivakumar, *Der Pharmacia Lettre*, 2011, **3**, 119–128.

11 T. A. Sherazi, in *Encyclopedia of Membranes*, ed. E. Drioli and L. Giorno, Springer Berlin Heidelberg, Berlin, Heidelberg, 2016, pp. 886–887.

12 R. B. Rohit, H. V. Gangadharappa, M. Afrasim, D. V. Gowda and M. O. Riyaz Ali, *Nat. Prod. J.*, 2015, **5**, 124–139.

13 L. Liu, W. Yao, Y. Rao, X. Lu and J. Gao, *Drug Delivery*, 2017, **24**, 569–581.

14 S. Zhuo, F. Zhang, J. Yu, X. Zhang, G. Yang and X. Liu, *Molecules*, 2020, **25**, 5064.

15 H.-W. Sung, K. Sonaje, Z.-X. Liao, L.-W. Hsu and E.-Y. Chuang, *Acc. Chem. Res.*, 2012, **45**, 619–629.

16 Z. Cao, W. Li, R. Liu, X. Li, H. Li, L. Liu, Y. Chen, C. Lv and Y. Liu, *Biomed. Pharmacother.*, 2019, **118**, 109340.

17 G. M. El-Mahrouk, M. H. Aboul-Einien and A. I. Makhlouf, *AAPS PharmSciTech*, 2016, **17**, 1285–1297.

18 V. Lavakumar, C. Sowmya, N. Venkateshan, V. Ravichandiran, K. Leela, N. Harikrishanan and J. Anbu, *Int. J. Pharm. Invest.*, 2018, **8**, 24.

19 T. Alam, S. Khan, B. Gaba, M. F. Haider, S. Baboota and J. Ali, *Drug Delivery*, 2017, **24**, 358–369.

20 G. Rena, D. G. Hardie and E. R. Pearson, *Diabetologia*, 2017, **60**, 1577–1585.

21 O. Horakova, P. Kroupova, K. Bardova, J. Buresova, P. Janovska, J. Kopecky and M. Rossmeisl, *Sci. Rep.*, 2019, **9**, 6156.

22 P. H. Marathe, M. E. Arnold, J. Meeker, D. S. Greene and R. H. Barbhaiya, *J. Clin. Pharmacol.*, 2000, **40**, 1494–1502.

23 L. J. McCreight, C. J. Bailey and E. R. Pearson, *Diabetologia*, 2016, **59**, 426–435.

24 M. Siavash, M. Tabbakhian, A. M. Sabzghabaee and N. Razavi, *J. Res. Pharm. Pract.*, 2017, **6**, 73–76.

25 R. R. Bhosale, H. V. Gangadharappa, R. A. M. Osmani and D. V. Gowda, *Drug Delivery Transl. Res.*, 2020, **10**, 1002–1018.

26 T. A. Afolabi and D. G. Adekanmi, *J. Polym.*, 2017, **2017**, 3125385.

27 G. Nandi, P. Patra, R. Priyadarshini, S. Kaity and L. K. Ghosh, *Int. J. Biol. Macromol.*, 2015, **72**, 965–974.

28 V. Vijan, S. Kaity, S. Biswas, J. Isaac and A. Ghosh, *Carbohydr. Polym.*, 2012, **90**, 496–506.

29 S. Kaity, J. Isaac, P. M. Kumar, A. Bose, T. W. Wong and A. Ghosh, *Carbohydr. Polym.*, 2013, **98**, 1083–1094.

30 D. J. Omrod, C. C. Holmes and T. E. Miller, *Atherosclerosis*, 1998, **138**, 329–334.

31 N. Lal, J. Dubey, P. Gaur, N. Verma and A. Verma, *Mater. Sci. Eng., C*, 2017, **79**, 491–498.

32 T. F. Vandamme, A. Lenourry, C. Charrueau and J. C. Chaumeil, *Carbohydr. Polym.*, 2002, **48**, 219–231.

33 H. Wei, F. Li-Fang, B. Min, C. Yong-Zhen, X. Bai, D. Qing, W. Feng, Q. Min and C. De-Ying, *J. Pharm. Sci.*, 2010, **99**, 186–195.

34 B. Vishwa, A. Moin, D. V. Gowda, S. M. D. Rizvi, W. A. H. Hegazy, A. S. Abu Lila, E.-S. Khafagy and A. N. Allam, *Pharmaceutics*, 2021, **13**, 79.

35 A. A. Hasan, R. M. Samir, S. S. Abu-Zaid and A. S. Abu Lila, *Colloids Surf., B*, 2020, **194**, 111208.

36 R. A. Osmani, P. K. Kulkarni, S. Shanmuganathan, U. Hani, A. Srivastava, M. Prerana, C. G. Shinde and R. R. Bhosale, *RSC Adv.*, 2016, **6**, 18737–18750.

37 P. Iriventi, N. V. Gupta, R. A. Osmani and V. Balamuralidhara, *Daru, J. Pharm. Sci.*, 2020, **29**, 1–8.

38 N. A. Qinna and A. A. Badwan, *Drug Des., Dev. Ther.*, 2015, **9**, 2515–2525.

39 M. P. Gowrav, U. Hani, H. G. Shivakumar, R. A. M. Osmani and A. Srivastava, *RSC Adv.*, 2015, **5**, 80005–80013.

40 T. K. Giri, P. Verma and D. K. Tripathi, *Adv. Compos. Mater.*, 2015, **24**, 531–543.

41 J. S. Karthika and B. Vishalakshi, *Int. J. Biol. Macromol.*, 2015, **81**, 648–655.

42 P. Kumar, A. L. Ganure, B. B. Subudhi and S. Shukla, *Drug Delivery Transl. Res.*, 2015, **5**, 243–256.

43 S. Muley, T. Nandgude and S. Poddar, *Asian J. Pharm. Sci.*, 2016, **11**, 684–699.

44 S. Ahuja and A. Kumar, *Int. J. Biol. Macromol.*, 2013, **61**, 411–415.

45 R. A. M. Osmani, N. H. Aloorkar, D. J. Ingale, P. K. Kulkarni, U. Hani, R. R. Bhosale and D. Jayachandra Dev, *Saudi Pharm. J.*, 2015, **23**, 562–572.

46 A. Srivastava, D. V. Gowda, U. Hani, C. G. Shinde and R. A. M. Osmani, *RSC Adv.*, 2015, **5**, 44652–44659.

47 T. Szkudelski, *Exp. Biol. Med.*, 2012, **237**, 481–490.

48 A. Poznyak, A. V. Grechko, P. Poggio, V. A. Myasoedova, V. Alfieri and A. N. Orekhov, *Int. J. Mol. Sci.*, 2020, **21**, 1835.